FR8602381

FRADOC--8-8

R1

FLAW ANALYSIS IN STEAM GENERATOR TUBE

HUTIN, J.P. Electricite de France, 75-Paris

BILLON, F. Framatome, 92-Paris-la-Defense (France)

Communication présentée à : 4. International seminar on assuring structural in integrity of steel reactor pressure boundary components

Ispra (Italy)

28-29 Aug 1985

FLAW ANALYSIS IN STEAM GENERATOR TUBE

Jean-Pierre HUTIN
ELECTRICITE DE FRANCE

François BILLON
FRAMATOME

1 - INTRODUCTION

Operating more than 30 PWR units, Electricité de France has to face several steam generator tube problems. One of the most serious difficulties is the stress corrosion cracking due to primary fluid, just above the tube sheet, in the roll transition region [1]. With regard to availability it is, of course, a major concern ; with regard to safety, the point is that tube rupture should be preceded by a significant primary-to-secondary leak during normal operation so that the reactor should be shut down before failure occurs. The demonstration of this assessment asks for experimental and analytical evidences. In 1981, Electricité de France started a comprehensive program on that subject. A general description of this program and the main results are to be presented during the SMIRT-8 Conference [2]. The purpose of the present paper is to develop in greater detail the analytical part of the work.

2 - METHODOLOGY

The main features of the analysis are : (1) evaluation of crack sizes (or lower bounds) which would lead to tube failure in various operating conditions (normal, upset, faulted and emergency) ; (2) evaluation of the leak rate through these critical size cracks during normal operation. These two points were investigated for through-wall longitudinal and circumferential cracks, in the lower part of tubes, either very close to the tube sheet ("transition zone") or far enough from it ("current zone").

Following burst test results, the most widely used failure criteria is based on plastic instability concept only : the applied opening stress, amplified by bulging, is compared to a flow stress limit [3,4]. However, difficulties arise when applying such criteria to actual operating conditions : thermal stresses, large stress gradients through the thickness, boundary conditions for circumferential cracks are uneasy to handle satisfactorily. More over, stable crack growth, observed during some experiments, is difficult to account for when using a pure plastic instability model. Then, it was felt to be more appropriate to chose a criteria which prevents from both plastic instability and ductile tearing initiation and which can cope with any stress state. So that the adopted criteria is quite similar to the CEGB R-6 approach [5].

.../...

The risk of failure of a cracked tube is assessed by positionning the point (K_R, S_R) in the Failure Assessment Diagram :

. K_R characterizes the risk of ductile tearing and is defined as :

$$K_R = K_{ICP}/K_{IJC}$$

K_{ICP} : mode I stress intensity factor with plastic zone correction

K_{IJC} : ductile tearing threshold (corresponding to J_{IC})

. S_R characterizes the risk of plastic instability and is defined as :

$$S_R = \sigma_A^m / \sigma_f$$

σ_A^m: applied membrane stress amplified by tube bulging

σ_f : flow stress

The limit curve in our diagram is the same as in the R-6 procedure. For giv n loading conditions, increasing the crack length drives the corresponding point in the Failure Assessment Diagram from inside the limit curve towards the outside. The intersection point corresponds to the critical size.

3 - STRESS ANALYSIS

Stresses induced by various operating conditions had to be estimated in the region of the tube where most cracking occurs i.e. just around the tube sheet upper face. For that purpose, a finite element model was prepared which represented the lower part of a tube and a part of the tube sheet. For the problem to remain axi-symetric, the tube sheet was modelized as two concentric solid annuli : one with actual material characteristics, immediately surrounding the tube ; the second one with equivalent mechanical properties to account for the holes. Four-nodes isoparametric elements were used with three elements in the tube thickness (fig. 1).

Loadings were : internal and external pressure, end force, primary and secondary temperature variations, displacement at the edge of the tube sheet, all taken out of the design transient list and stress report. Imposed displacements of the tube upper end were also investigated.

For normal and upset conditions, the following transients were selected : heat-up and cool-down, normal load variation, load step, loss of electrical power, hot stand-by fluctuations, steam generator level corrections, overcooling and overpressurisation transient.

Three accidental conditions were analyzed : loss of primary coolant accident (LOCA), steamline break (SLB), feed water line break (FWLB). A sophisticated thermohydraulic model, validated by inservice measurements, allowed to account for the warming up of feed water when it flows from the feed ring down to the tube sheet. In some cases, stresses were estimated using transfer functions derived from separate elementary loading analysis.

Calculations were also performed to represent burst test conditions.

.../...

It is worth noticing that special attention is necessary when analysing stresses in the tube just below the tubesheet upper face. In the finite element model, tube and tubesheet are in contact and the deformations due to internal pressure are restricted. But, in fact, the temperature field is such that this contact is lost in the last few millimeters so that the pressure-induced strains may develop freely. The solution was to consider that the actual pressure stresses at a distance d above the last point of contact was equal to the calculated pressure stresses at the distance d above the tube sheet in the finite element model.

4 - MATERIAL CHARACTERISTICS

In this "leak-before-break" analysis, conservatism was enhanced by considering minimum specified values of the material properties.

The limit value J_{IC} (threshold for ductile tearing initiation) was estimated from experimentally determined $J-\Delta a$ curves and assuming a blunting line equation $J = 4.\sigma_f.\Delta a$

K_{IJC} is related to J_{IC} through :

$$K_{IJC} = (E.J_{IC})^{1/2}$$

The flow stress value σ_f was conventionnaly taken equal to $\frac{1}{2}(\sigma_y + \sigma_u)$

Tests and experiments brought evidence of the conservatism associated with these various limiting values.

5 - CRITICAL CRACK SIZE ESTIMATE

5.1 - Parameter derivation for through-wall longitudinal crack in the current zone

The methodology described in paragraph 2 was applied. The corrected stress intensity factor K_{ICP} was derived as follows :

$$K_{ICP} = M_c . \sigma_c^m . \sqrt{\pi(a + r_y)} + \lambda_c (\sigma_c^{i,e} - \sigma_c^m).\sqrt{\pi(a + r_y)} \qquad (1)$$

σ_c^m: circumferential membrane stress

$\sigma_c^{i,e}$: I.D. or O.D. circumferential peak stress (whichever is the largest)

a : half crack length

r_y : plastic zone size

λ_c: circumferential peak stress participation factor $(= 1)$

M_c: bulging factor to be applied on circumferential stress and depending on tube dimensions and crack length.

The crack tip plasticity was supposed to be related to the membrane stress intensity factor :

$$r_y = \frac{1}{2\pi} \left(\frac{K_I^m}{\sigma_f} \right)^2 \qquad (2)$$

where $K_I^m = M_c . \sigma_c^m \sqrt{\pi a}$

For S computation, the amplified applied stress was :

$$\sigma_{A,c}^{m} = M_c \cdot \sigma_c^{m}$$

The various loading parameters σ_c^m, σ_c^i, σ_c^e do not reach their maximum value at the same time. So that all instants where one of them was maximum were selected. The corresponding K_R and S_R values were computed and the most severe solution was kept.

5.2 - Parameter derivation for through-wall circumferential crack in the current zone

The corrected stress intensity factor is defined as :

$$K_{ICP} = M_L \cdot \sigma_L^m \sqrt{\pi(a+r_y)} + \lambda_L \left(\sigma_L^{i,e} - \sigma_L^m\right)\sqrt{\pi(a+r_y)} \qquad (3)$$

σ_L^m : longitudinal membrane stress

$\sigma_L^{i,e}$: I.D. or O.D. longitudinal peak stress (whichever is the largest)

a : half crack length

r_y : plastic zone size associated with membrane stress intensity factor as in paragraph 5.1

λ_L : longitudinal peak stress participation factor $(=1)$

M_L : bulging factor to be applied on longitudinal stress and depending on tube dimensions and crack length

The amplified applied stress used in S_R computation is, in fact, a net section stress :

$$\sigma_{A,L}^{m} = M_L \cdot \sigma_L^{m} \cdot \frac{A_0}{A_R}$$

with A_0 : tube cross section

A_R : remaining tube cross section

5.3 - Parameter derivation in the transition zone

The procedure described in paragraph 5.1 had to be modified for longitudinal cracks in the transition region. Indeed, when the cracked part of a tube is completely or partly within the tube sheet, its bulging is restricted and so is the leak and the break capability. Then, only the length of the "emerging" part was considered and called the "effective" length a_{eff}.

The proximity of the tube sheet induces a longitudinal stress gradient so that, when applying equation 1, the membrane stress was taken as the average value on the effective crack length :

$$\overline{\sigma_c^m} = \frac{1}{2a_{eff}} \cdot \int_0^{2a_{eff}} \sigma_c^m(z) \cdot dz$$

However, for the peak stress, the value at the upper crack tip level was considered.

5.4 - Critical crack sizes

For each selected transient, the parameters K_R and S_R were calculated for various crack lengthes and the associated points were plotted in the failure assessment diagram. Points falling on the limit curve corresponded to critical crack sizes.

The most severe transient appears to be the feedwater line break when the cracked tube is in the affected steam generator. Analysis results for this accident are shown as example in figure 2 and 3 : in the current zone, the critical size is around 16 mm for longitudinal cracks and more than 180° for circumferential cracks (fig. 2) ; in the transition zone, the critical "effective"size is around 16.5 mm for longitudinal cracks and more than 180° for circumferential cracks (fig. 3).

It may be worth recalling that these values are lower bounds of the critical size because of the conservatism associated with the models and data, particularly for material properties.

6 - LEAK RATE ESTIMATE

6.1 - Position of the problem

The point is to demonstrate that, before reaching a critical size, a crack will induce a significant leak during normal operation. This implies to be able to estimate the leak rate through a given through-wall crack under nominal pressure. For that purpose, test results and experimental evidences plaid a major part ; however, analysis was also called for in order to compute crack opening areas.

6.2 - Longitudinal cracks in the current zone

Finite element technique was used again, with three-dimension models, 20 node elements and quarter-side nodes for the elements surrounding the crack tips. The mesh was optimized through calculation of a cracked plate and comparison with analytical solution. Crack edge displacements were evaluated for various crack lengthes under several elementary loadings : internal pressure, external pressure, pressure on the crack faces.

These displacements were found to be in good agreement with solutions proposed by Erdogan [6]. In the same manner, the stress intensity factors derived from computed displacements compared well with the "bulging factor" formulation of paragraph 5.1.

The leak area was then calculated by integrating second order polynomials fitting the deformation of each element side. Results are consistent with Kastner solutions [7]. Inside and outside crack edges were considered successively. An example of deformed mesh is shown in figure 4.

6.3 - Circumferential cracks

For circumferential cracks, a shell model was used with sufficient extension to correctly take in account the first support plate and the tube sheet. Eight-node elements were adopted with quarter-side nodes for elements surrounding the crack tips. Several elementary loadings were separately considered : internal and external pressure, pressure on the crack faces, end force, imposed displacement at the support plate level, imposed rotation of the tube sheet.

Again, the various results compare well with already published solutions [6, 7]. Attention must be paid to the fact that the crack lower edge displacements may not be symetric of the upper edge ones, due to the proximity of the tube sheet. An example of deformed mesh is shown in figure 4.

6.2 - Longitudinal cracks in the transition zone

For cracks which are partly below the tube sheet upper face, it is necessary to account for the restraining effect of the tube sheet. This was obtained as follows :

- Only the emerging part of the crack was considered like in the failure analysis ("effective length" concept).

- The crack was supposed to be opened by an equivalent differential pressure ΔP^* defined as :

$$\overline{\sigma}_c^m = \frac{\Delta P^* . R}{t}$$

where $\overline{\sigma}_c^m$ is the calculated average circumferential membrane stress (see paragraph 5.3), R is mean tube radius and t is nominal tube thickness.

6.3 - Plasticity correction

It was felt to be necessary to take in account the plasticity which develops in the vicinity of the crack tip. For that purpose, a correction was proposed which is similar to Irwin plastic zone correction currently used for stress intensity factor evaluation.

So that, for a crack length 2 a, the leak area was elastically computed assuming a fictitious crack length 2 a + $2r_y$ in which r_y was the plastic zone radius defined as :

$$r_y = \frac{1}{2\pi} \cdot \left(\frac{K_I}{\sigma_f} \right)^2$$

6.4 - Results

From the leak area, the leak rate could be calculated using the following relation :

$$Q = K.S.\sqrt{2\Delta P/\rho}$$

Q : leak rate

K : experimentally determined coefficient (around 0.3)

S : leak area

ΔP : differential pressure

ρ : fluid density

Results of the leak rate calculations are shown in figure 5.

7 - CONCLUSION

Although evidences brought by the experimental part of the program plays a major part, sophisticated analytical work was also necessary to get to the conclusion that, indeed, tube rupture due to stress corrosion cracks should be preceded by significant primary-to-secondary leakage.

REFERENCES

1 - DAURES N., "French Steam Generator Experience reviewed", Nuclear Engineering International, November 1984

2 - HUTIN J.P., BILLON F., "Integrity Analysis of Cracked Steam Generator Tubes", SMIRT-8 Conference, paper G 6/5, Bruxelles, 1985

3 - HERNALSTEEN P., "Evaluation of Critical Sizes for Defects in Small Diameter Tubing", SMIRT-7 Conference, Paper GF 4/3, Chicago, 1983

4 - BERGE, CATTANT, CALLE, HUTIN, "Characteristics of roll transition cracks in steam generator tubes", NEA-CSNI-UNIPEDE Specialist Meeting, Stockholm, October 1984

5 - HARRISON, LOOSEMORE, MILNE, "Assessment of the Integrity of Structures Containing Defects", CEGB Report R-H-R6, U.K., 1976

6 - ERDOGAN F., RATWANI M., "Fracture of cylindrical and spherical shells containing a crack", Nuclear Engineering and Design, 20, 1972

7 - KASTNER W. and al., "Critical crack sizes in ductile piping", Int. J. Pressure Vessel and Piping, 9, 1981.

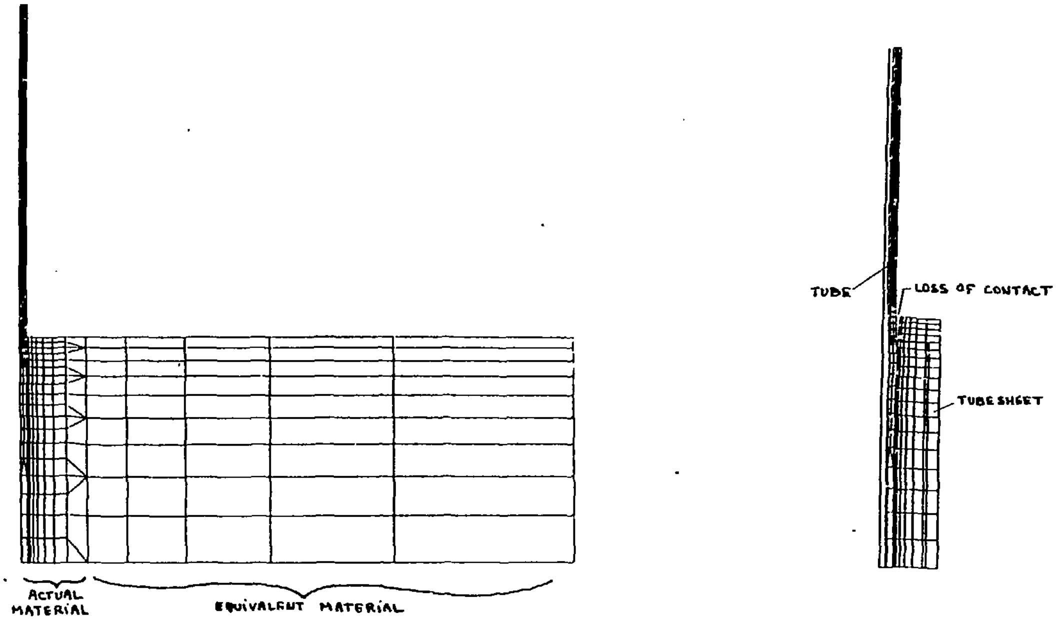

a - No loading

b - with thermal loading

Figure 1 - Finite element model of tube and tube sheet for stress analysis

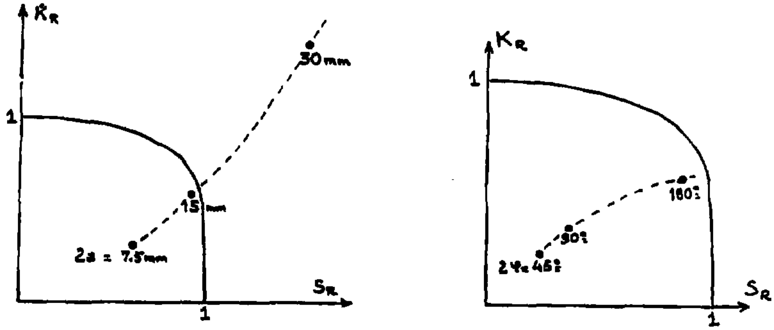

a - Longitudinal crack   b - Circumferential crack

Figure 2 - Failure assessment diagram for cracks in the current zone during feedwater line break

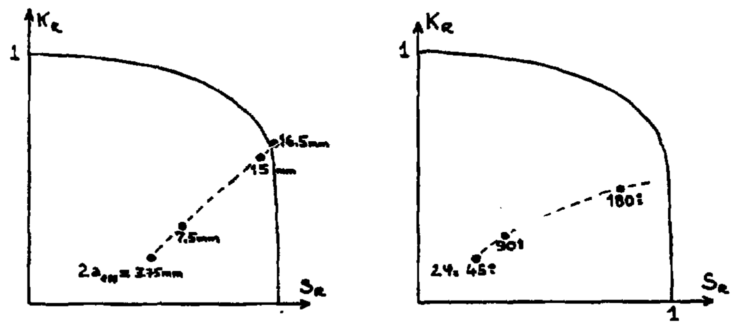

a - Longitudinal crack   b - Circumferential crack

Figure 3 - Failure assessment diagram for cracks in the transition zone during feedwater line break

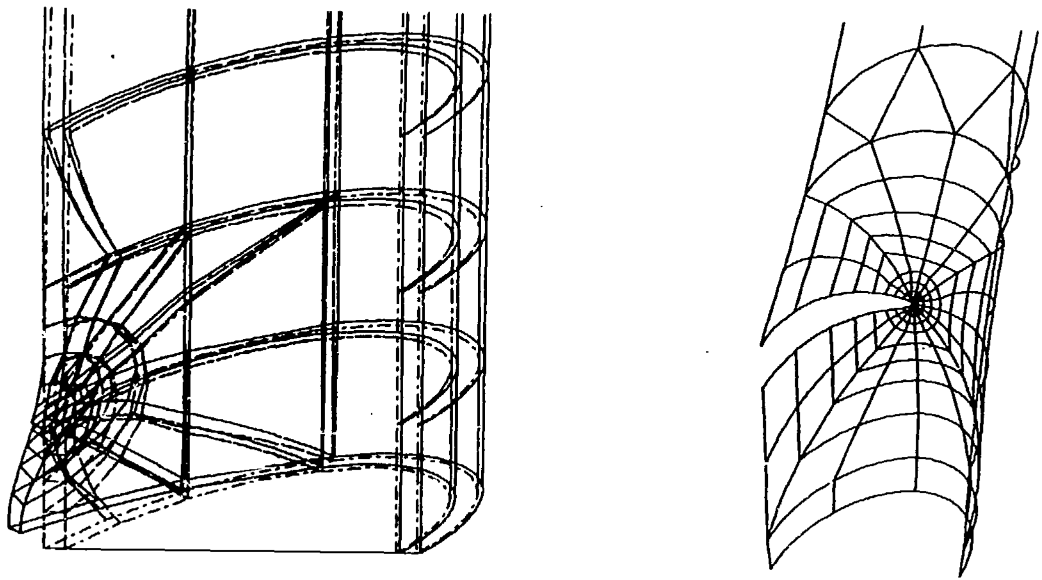

a - Longitudinal crack under pressure

b - circumferential crack under pressure

Figure 4 - Finite element model for leak area calculation

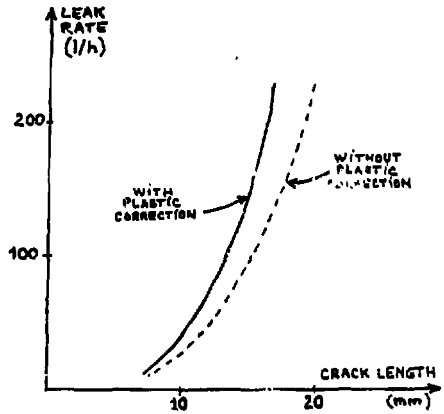

a - Longitudinal cracks

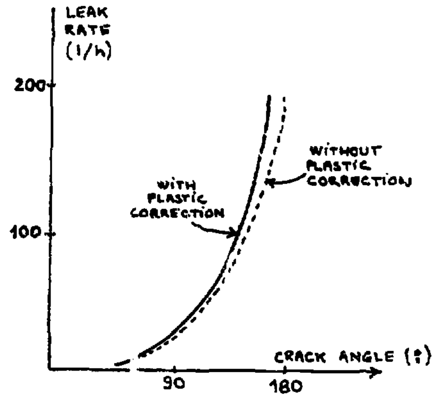

b - Circumferential cracks

Figure 5 - Calculated leak rates during normal operation through crack in the current zone